Parity Violation

DOI: 10.1002/anie.201406071

High-Resolution Spectroscopy of the Chiral Metal Complex [CpRe(CH_3)(CO)(NO)]: A Potential Candidate for Probing Parity Violation**

*Chris Medcraft, Robert Wolf, and Melanie Schnell**

Abstract: *Heavy-metal containing chiral compounds have been suggested as promising candidates for studying parity-violation effects. We report herein the broadband rotational spectroscopy study of the chiral complex [CpRe(CH_3)(CO)(NO)] in the gas phase. The spectra obtained are very rich due to the two rhenium isotopologues (^{185}Re and ^{187}Re), hyperfine structure arising from the rhenium and nitrogen nuclei, and the asymmetry of the chiral complex. Since rhenium is located very close to the molecular center of mass, the rotational constants for the two rhenium isotopologues are very similar. However they can be differentiated by their characteristic nuclear quadrupole hyperfine splitting patterns. Comparison with calculated nuclear quadrupole coupling constants shows that all-electron relativistic basis sets are necessary for a correct description of the rhenium atom in this type of complex. The present study is an important step towards future precision studies on chiral molecules.*

Chirality is a fundamentally important molecular property because enantiomers of the same molecules show dramatically different chemical reactivity and biological functionality in a homochiral environment, such as nature. While the (bio)chemical properties of the enantiomers can be dramatically different, their physical properties (such as boiling and melting points) are to a very good approximation identical. However, parity violation induced by the weak force affects the molecular energy-level structure of chiral molecules, leading to an overall energy difference between the enantiomers,[1,2] which was first discussed by Rein and Letokhov in the mid-1970s.[3,4] This small energy difference is discussed as a possible cause for the homochirality of life on earth.[5–7] It has not yet been experimentally observed in molecules but it is predicted to increase for molecules containing heavy nuclei close to the stereogenic center of the molecule.[8] Recently, heavy-metal-containing chiral compounds, such as the rhenium complexes [CpRe(CO)(NO)X] (X = H, Cl, I), have been suggested as potential candidates for precision experiments aimed at determining this small energy difference.[9–11] For example, the calculated energy difference between the enantiomers of [CpRe(CO)(NO)I] amounts to about 300 Hz.

With the present rotational spectroscopy study of chiral, [CpRe(CH_3)(CO)(NO)] (Cp = η^5-cyclopentadienyl), we lay the foundation for upcoming studies on parity violation, such as those based on high-resolution infrared and microwave spectroscopy.[11,12] To our knowledge, this is the first high-resolution microwave spectroscopy study of a chiral organometallic complex of this type. To date, only a few achiral molecules of this type, such as [HRe$(CO)_5$],[13] [CpRe$(CO)_3$],[14] [(CH_3)Re(C_2H_2)O_2],[15] and [(CH_3)ReO_3],[16] have been studied with high-resolution microwave spectroscopy.

In comparison with the previously studied molecules, [CpRe(CH_3)(CO)(NO)] has four different ligands coordinated to the central rhenium atom. Both the Cp and the methyl groups can, in principle, perform internal rotations with respect to the remaining of the molecule that would lead to characteristic line patterns in our spectra. Furthermore, both naturally occurring rhenium isotopes and ^{14}N have a nuclear spin $I \geq 1$ ($I_{\mathrm{Re}} = 5/2$ and $I_{\mathrm{N}} = 1$), which leads to significant hyperfine structure in the spectrum as a result of the coupling of the nuclear spins with the overall rotation of the molecule. The magnitude of the hyperfine splitting reflects the anisotropy in the electric-field gradient surrounding the quadrupolar nucleus, which can be used to describe the bonding situation in the vicinity of the respective nuclei. This can be compared with other molecules and with calculated electronic properties.[17]

We use broadband rotational spectroscopy to investigate the rotational spectrum of racemic [CpRe(CH_3)(CO)(NO)] in the gas phase using the Hamburg chirped-pulse Fourier transform microwave (CP-FTMW) spectrometer COMPACT that has been detailed elsewhere.[18] Rotational spectra can provide detailed information about structural and electronic molecular properties, as well as insight into intramolecular dynamics, such as internal rotation. The broadband spectrometer covers the 2–8.5 GHz frequency range and is thus particularly suited for larger and heavier molecules that have large moments of inertia and therefore small rotational

---

[*] Dr. C. Medcraft, Priv.-Doz. Dr. M. Schnell
Max-Planck-Institut für Struktur und Dynamik der Materie
Luruper Chaussee 149, 22761 Hamburg (Germany)
and
Center for Free-Electron Laser Science
Luruper Chaussee 149, 22761 Hamburg (Germany)
E-mail: melanie.schnell@mpsd.mpg.de
Prof. Dr. R. Wolf
Universität Regensburg, Institut für Anorganische Chemie
Universitätsstrasse 31, 93053 Regensburg (Germany)

[**] We acknowledge funding by the Deutsche Forschungsgemeinschaft for Sachbeihilfe SCHN1280/1-1 and the Fonds der Chemischen for a Dozentenstipendium for M.S. This work has also been supported by Die Junge Akademie (M.S. and R.W.) and the excellence cluster "The Hamburg Centre for Ultrafast Imaging—Structure, Dynamics and Control of Matter at the Atomic Scale" of the Deutsche Forschungsgemeinschaft. R.W. would like to thank D. Herrmann, C. Hoidn, D. Paul, and S. Pelties for assistance in preparing chiral rhenium complexes.

Supporting information for this article is available on the WWW under http://dx.doi.org/10.1002/anie.201406071.

constants, such as [CpRe(CH_3)(CO)(NO)]. The microwave chirp spanning several GHz in only a few microseconds is employed to excite the molecules, combined with broadband detection using a fast digital oscilloscope. Our spectrometer is equipped with a pulsed source for supersonically expanding the [CpRe(CH_3)(CO)(NO)] molecules into vacuum. The complex was synthesized following the procedure described in Ref. [19]. It was heated in a sample holder to about 105 °C to generate sufficient vapor pressure, which is then diluted by neon as an inert carrier gas and subsequently supersonically expanded. More experimental details are given in the Supporting Information.

Table 1: Molecular parameters for [CpRe(CH_3)(CO)(NO)]. All values are given in MHz.

Molecular parameters	^{187}Re experiment	^{187}Re theory[a]	^{185}Re experiment	^{185}Re theory[a]	Ratio ^{185}Re/^{187}Re experiment
A	1232.1883(107)	1232.70	1232.2187(128)	1232.73	1.00003
B	897.20692(88)	878.27	897.23098(101)	878.30	1.00003
C	749.82214(62)	740.21	749.83700(75)	740.23	1.00002
$\chi_{aa}{}^{(Re)}$	681.555(39)	641.31	720.210(61)	675.37	1.057
$\chi_{bb}{}^{(Re)}$	−202.391(71)	−305.39	−216.065(75)	−321.59	1.056
$\chi_{cc}{}^{(Re)}$	−477.165(71)	−335.92	−504.145(75)	−353.78	1.056
$\sim\chi_{ab}{}^{(Re)}$	348.203(203)	282.68	368.39(81)	297.74	1.058
$\sim\chi_{bc}{}^{(Re)}$	119.308(208)	62.70	120.27(172)	66.02	1.09
χ_{aa} (^{14}N)	0.560(35)	0.60	0.475(40)	0.61	0.60
χ_{bb} (^{14}N)	0.387(38)	0.46	0.446(58)	0.46	1.026
χ_{cc} (^{14}N)	−0.947(38)	−1.06	−0.921(58)	−1.06	1.026
Number of transitions	172	–	130	–	
rms error	0.020	–	0.016	–	

[a] For the ab initio calculations, the B3LYP density functional employing the Douglas–Kroll–Hess Hamiltonian has been used with an ANO-RCC basis set for the rhenium site and a cc-pVQZ basis set for the lighter atoms (H, C, N, and O).

The rotational spectrum of [CpRe(CH_3)(CO)(NO)] from 3–8 GHz is shown in Figure 1 (top trace), along with its global minimum structure obtained from density functional theory (B3LYP) optimizations. In our frequency range, we cover four a-type rotational transitions denoted by the rotational quantum numbers J, K_a, and K_c, with J being the rotational angular momentum quantum number and K_a and K_c the projections of J onto the principal rotational axes of the molecules at the prolate and oblate symmetric top limits, respectively. The rotational transitions show a rich substructure due to the presence of the two rhenium isotopologues in natural abundance (^{185}Re (37.4 %), Figure 1 blue trace, and ^{187}Re (62.6 %), red trace) and due to the rhenium and nitrogen nuclear quadrupole coupling, which is shown in more detail in Figure 2 and Figure 3 and discussed below. A detailed knowledge of the nuclear quadrupole hyperfine structure is crucial for subsequent precision measurements on parity violation. Note that no additional line splittings arising from internal rotation of the Cp and the methyl group have been observed, in agreement with the calculated barrier heights, which is discussed in more detail in the Supporting Information.

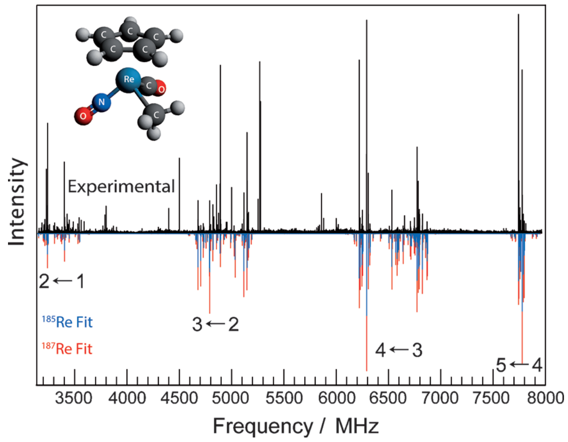

Figure 1. Broadband rotational spectrum. Top trace: 3–8 GHz, average of 50 000 individual measurements. Bottom trace: simulated spectra based on the fitted values reported in Table 1, and equilibrium structure of [CpRe(CH_3)(CO)(NO)]. The four rotational transitions are denoted with their respective J quantum numbers. The richness of the spectrum arises from the two rhenium isotopologues, the K substructure, and the rhenium and the nitrogen hyperfine structures.

The magnitudes of the nuclear quadrupole moments of the rhenium and nitrogen nuclei differ by more than two orders of magnitude. As a result, each rotational transition is first split into several rhenium hyperfine transitions and each of these transitions is split on a smaller scale by coupling with the nitrogen quadrupole. The observed splittings are very characteristic and can be used to identify different rhenium isotopologues despite their rotational constants being very similar. Initial assignment and fitting of rotational transitions was performed using the PGOPHER program package.[20] These were then refined using Pickett's CALPGM program suite[21] utilizing Watson's A-reduced Hamiltonian in the I^r representation. The nuclear quadrupole coupling was described by the sequential spin coupling scheme, $J + I_{Re} = F_1$ and $F_1 + I_N = F$, where I is the nuclear spin of the rhenium or nitrogen, and F is the total angular momentum.[22] The molecular parameters obtained from these fits are summarized for both isotopologues in Table 1 along with ab initio values calculated at the B3LYP level of theory employing the Douglas–Kroll–Hess Hamiltonian and utilizing the cc-pVQZ basis set for the light atoms and the atomic natural orbital relativistic core correlation (ANO-RCC) basis set[23] for the rhenium atom, in the Gaussian 09 program package.[24] The simulated spectrum based on the fitted values is given in the bottom trace of Figure 1. SPFIT output files and computational details are given in the Supporting Information.

An expanded view of the $(J+1)_{K'_aK'_c} \leftarrow J_{K_aK_c} = 5_{05} \leftarrow 4_{04}$ rotational transition is given in Figure 2. It shows the large overlap between the two isotopologues. The dominant substructure arises from rhenium nuclear quadrupole coupling. Each rhenium hyperfine transition is further split as a result of nitrogen quadrupole coupling, as shown in the inset of

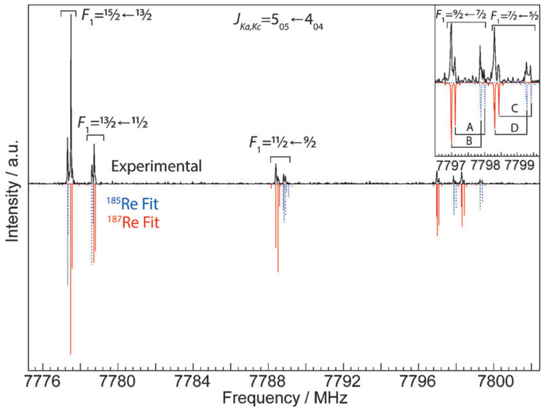

Figure 2. Rhenium hyperfine structure for the $(J+1)_{K'_aK'_c} \leftarrow J_{K_aK_c} = 5_{05} \leftarrow 4_{04}$ rotational transition. The characteristic splitting because of the rhenium nuclear quadrupole coupling differs for the two rhenium isotopologues. ^{187}Re (red, solid line), ^{185}Re (blue, dashed line). Note that every rhenium hyperfine component of a rotational transition is further split by nitrogen nuclear quadrupole coupling. This splitting is shown in the inset for the $F_1 = 9/2 \leftarrow 7/2$ and $F_1 = 7/2 \leftarrow 5/2$ rhenium hyperfine transitions, with A: $F = 11/2 \leftarrow 9/2$ and $F = 7/2 \leftarrow 5/2$ (not resolved), B: $F = 9/2 \leftarrow 7/2$, C: $F = 9/2 \leftarrow 7/2$, and $5/2 \leftarrow 3/2$, D: $F = 7/2 \leftarrow 5/2$. Where $F = F_1 + I_N$ and $F_1 = J + I_{Re}$.

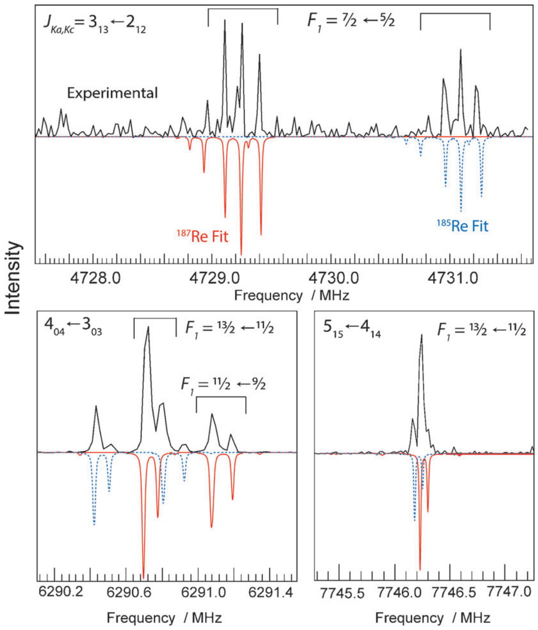

Figure 3. Nitrogen hyperfine structure of [CpRe(CH$_3$)(CO)(NO)] for three different rotational transitions. The nuclear quadrupole splitting decreases with increasing rotational quantum number J. Top trace is experimental data, lower traces are simulations based on fitted parameters. ^{187}Re (red, solid line), ^{185}Re (blue, dashed line).

Figure 2 and in Figure 3 for the $3_{13} \leftarrow 2_{12}$, $4_{04} \leftarrow 3_{03}$, and the $5_{15} \leftarrow 4_{14}$ rotational transitions. The rhenium nuclear quadrupole hyperfine structure is significantly different for the ^{185}Re and ^{187}Re isotopologues. This is directly visible in the spectra (Figure 2): the low-frequency ^{185}Re transitions are located at lower frequencies than the same transitions from the ^{187}Re isotopologue, this is reversed for the higher frequency components, pointing to the smaller overall splitting of ^{187}Re. This observation is in accordance with the atomic values ($Q(^{185}\mathrm{Re}) = +218.0(20)$ fm^2 and $Q(^{187}\mathrm{Re}) = +207.0(20)$ fm^2). The clear difference allows us to unambiguously distinguish the two rhenium isotopologues. Usually, isotopologues are distinguished on the basis of their rotational constants. However, for [CpRe(CH$_3$)(CO)(NO)] the rhenium atom is located very close to the center of mass of the molecule so that the resulting rotational constants are nearly identical (Table 1) and differentiation is not possible based on these values alone.

A significant portion of the rhenium quadrupole coupling arises from the off-diagonal elements of the quadrupole tensor, χ_{ab} and χ_{bc}, which usually do not play notable roles. The effect of the off-diagonal terms in [CpRe(CH$_3$)(CO)(NO)] is so large that the components of the rotational transitions could not be fitted to experimental values without them. The mean errors obtained from fits without any off-diagonal elements were approximately 1.7 MHz. The stepwise inclusion of χ_{ab} and χ_{bc} reduces the error to 0.5 MHz and 0.02 MHz, respectively, with only a slight additional improvement when χ_{ac} is also included. The fitted value of χ_{ac} is about 1 MHz, which is smaller than its standard deviation, therefore χ_{ac} is not included in the final fit in Table 1.

The nitrogen nuclear quadrupole hyperfine splittings are shown in Figure 3 for three different rotational transitions with increasing rotational quantum number J. With increasing J, the splitting gets more congested, which is typical for nuclear quadrupole coupling.

The nuclear quadrupole coupling constants can provide information about the electronic environment of the respective nuclei, particularly when similar molecules are compared. However, in this case the difference in symmetry between previously studied molecules and the presence of large off-diagonal elements make a direct quantitative comparison difficult. But it is worth noting that the order of magnitude of χ_{aa} for [CpRe(CH$_3$)(CO)(NO)] is the same as for the previously investigated symmetric-top molecules [CpRe(CO)$_3$] and [(CH$_3$)ReO$_3$] (see Table S1 of the Supporting Information). Insights into the chemical environment at the nitrogen atom are also problematic as the bonds are not along any symmetric axis.

High-resolution rotational spectroscopy is a powerful way to precisely determine the structures of polar molecules in the gas phase, as for example recently shown for strawberry aldehyde and the sevoflurane-benzene complex.[25,26] The position of each individual atom with respect to the molecule's center of mass and thus its structure can be determined by isotopic substitution. In the present study, we cannot directly extract detailed structural parameters from our experimental data since we did not observe other isotopologues besides the ones of rhenium and in particular no ^{13}C isotopologues, but we can compare the experimental molecular parameters with those from quantum chemical structure calculations. Rotational constants are very sensitive to structural changes, so that a good agreement between experiment and theory gives us further confidence in the optimized structural parameters.

In summary, we investigated the chiral heavy-metal containing complex [CpRe(CH_3)(CO)(NO)] using high-resolution broadband rotational spectroscopy in the gas phase, which is a promising candidate for studying parity violation effects in chiral molecules. It shows a rich spectrum as a result of the two rhenium isotopologues [Cp^{185}Re(CH_3)(CO)(NO)] and [Cp^{187}Re(CH_3)(CO)(NO)], the widely split rhenium hyperfine structure, and the nitrogen hyperfine structure. Even though the rotational constants are very similar for the two isotopologues since the rhenium atom is located very close to the molecular center of mass, we can differentiate between the isotopologues based on their characteristic hyperfine splitting patterns. Comparison with calculated nuclear quadrupole coupling coefficients clearly indicates that relativistic effects are inherently necessary for a correct description of rhenium in this type of complexes. Our spectra do not resolve effects from internal motions of the Cp or the methyl group, in agreement with results from ab initio calculations. With this detailed high-resolution rotational spectroscopy study of [CpRe(CH_3)(CO)(NO)], we demonstrate that such asymmetric molecules can be investigated in the gas phase and provide detailed spectroscopic properties. This knowledge is an important requirement for upcoming precision studies on such chiral heavy-metal containing compounds, employing well-controlled, slow molecular beams and high-resolution spectroscopy setups.

Received: June 10, 2014

Keywords: chirality · chirped-pulse Fourier-transform rotational spectroscopy · microwave spectroscopy · nuclear quadrupole coupling · parity violation

---

[1] "The Search for Parity Violation in Chiral Molecules": P. Schwerdtfeger in *Computational Spectroscopy* (Ed.: J. Grunenberg), Wiley-VCH, Weinheim, **2010**.
[2] M. Quack, J. Stohner, M. Willeke, *Annu. Rev. Phys. Chem.* **2008**, *59*, 741–769.
[3] D. Rein, *J. Mol. Evol.* **1974**, *4*, 15–22.
[4] V. Letokhov, *Phys. Lett. A* **1975**, *53*, 275–276.
[5] R. Wesendrup, J. K. Laerdahl, R. N. Compton, P. Schwerdtfeger, *J. Phys. Chem. A* **2003**, *107*, 6668–6673.
[6] W. A. Bonner, *Chirality* **2000**, *12*, 114–126.
[7] M. Quack, *Angew. Chem. Int. Ed.* **2002**, *41*, 4618–4630; *Angew. Chem.* **2002**, *114*, 4812–4825.
[8] J. K. Laerdahl, P. Schwerdtfeger, *Phys. Rev. A* **1999**, *60*, 4439–4453.
[9] P. Schwerdtfeger, J. Gierlich, T. Bollwein, *Angew. Chem. Int. Ed.* **2003**, *42*, 1293–1296; *Angew. Chem.* **2003**, *115*, 1331–1334.
[10] P. Schwerdtfeger, R. Bast, *J. Am. Chem. Soc.* **2004**, *126*, 1652–1653.
[11] B. Darquie, C. Stoeffler, S. Zrig, J. Crassous, P. Soulard, P. Asselin, T. R. Huet, L. Guy, R. Bast, T. Saue, P. Schwerdtfeger, A. Shelkovnikov, C. Daussy, A. Amy-Klein, C. Chardonnet, *Chirality* **2011**, *22*, 870–884.
[12] M. Schnell, J. Küpper, *Faraday Discuss.* **2011**, *150*, 33–49.
[13] S. G. Kukolich, S. M. Sickafoose, *J. Chem. Phys.* **1993**, *99*, 6465–6469.
[14] B. J. Drouin, P. A. Cassak, S. G. Kukolich, *J. Chem. Phys.* **1998**, *108*, 8878–8883.
[15] S. G. Kukolich, B. J. Drouin, O. Indris, J. J. Dannemiller, J. P. Zoller, W. A. Herrmann, *J. Chem. Phys.* **2000**, *113*, 7891–7900.
[16] P. Wikrent, B. J. Drouin, S. G. Kukolich, J. C. Lilly, M. T. Ashby, W. A. Herrmann, W. Scherer, *J. Chem. Phys.* **1997**, *107*, 2187–2192.
[17] M. Schnell, J.-U. Grabow, *Angew. Chem. Int. Ed.* **2006**, *45*, 3465–3470; *Angew. Chem.* **2006**, *118*, 3544–3549.
[18] D. Schmitz, V. A. Shubert, T. Betz, M. Schnell, *J. Mol. Spectrosc.* **2012**, *280*, 77–84.
[19] J. R. Sweet, W. A. G. Graham, *J. Am. Chem. Soc.* **1982**, *104*, 2811–2815.
[20] C. M. Western, *PGOPHER, A Programm for Simulation Rotational Structure*, http://pgopher.chm.bris.ac.uk.
[21] H. M. Pickett, *J. Mol. Spectrosc.* **1991**, *148*, 371–377.
[22] H. Benz, A. Bauder, H. Günthard, *J. Mol. Spectrosc.* **1966**, *21*, 156–164.
[23] D. A. Pantazis, X.-Y. Chen, C. R. Landis, F. Neese, *J. Chem. Theory Comput.* **2008**, *4*, 908–919.
[24] M. J. Frisch, G. W. Trucks, H. B. Schlegel, G. E. Scuseria, M. A. Robb, J. R. Cheeseman, G. Scalmani, V. Barone, B. Mennucci, G. A. Petersson, H. Nakatsuji, M. Caricato, X. Li, H. P. Hratchian, A. F. Izmaylov, J. Bloino, G. Zheng, J. L. Sonnenberg, M. Hada, M. Ehara, K. Toyota, R. Fukuda, J. Hasegawa, M. Ishida, T. Nakajima, Y. Honda, O. Kitao, H. Nakai, T. Vreven, J. A. Montgomery, J. E. Peralta, F. Ogliaro, M. Bearpark, J. J. Heyd, E. Brothers, K. N. Kudin, V. N. Staroverov, R. Kobayashi, J. Normand, K. Raghavachari, A. Rendell, J. C. Burant, S. S. Iyengar, J. Tomasi, M. Cossi, N. Rega, J. M. Millam, M. Klene, J. E. Knox, J. B. Cross, V. Bakken, C. Adamo, J. Jaramillo, R. Gomperts, R. E. Stratmann, O. Yazyev, A. J. Austin, R. Cammi, C. Pomelli, J. W. Ochterski, R. L. Martin, K. Morokuma, V. G. Zakrzewski, G. A. Voth, P. Salvador, J. J. Dannenberg, S. Dapprich, A. D. Daniels, Farkas, J. B. Foresman, J. V. Ortiz, J. Cioslowski, D. J. Fox, *Gaussian 09*, Wallingford CT, **2009**..
[25] S. T. Shipman, J. L. Neill, R. D. Suenram, M. T. Muckle, B. H. Pate, *J. Phys. Chem. Lett.* **2011**, *2*, 443–448.
[26] N. A. Seifert, D. P. Zaleski, C. Perez, J. L. Neill, B. H. Pate, M. Vallejo-Lopez, A. Lesarri, E. J. Cocinero, F. Castano, I. Kleiner, *Angew. Chem. Int. Ed.* **2014**, *53*, 3210–3213; *Angew. Chem.* **2014**, *126*, 3274–3277.